

## Kelvin waves with helical Beltrami flow structure

Rafael González, Gustavo Sarasua, and Andrea Costa

Citation: *Physics of Fluids* (1994-present) **20**, 024106 (2008); doi: 10.1063/1.2840196

View online: <http://dx.doi.org/10.1063/1.2840196>

View Table of Contents: <http://scitation.aip.org/content/aip/journal/pof2/20/2?ver=pdfcov>

Published by the [AIP Publishing](#)

---

### Articles you may be interested in

[Decay of helical Kelvin waves on a quantum vortex filament](#)

*Phys. Fluids* **26**, 075101 (2014); 10.1063/1.4887519

[Weak turbulence of Kelvin waves in superfluid He](#)

*Low Temp. Phys.* **36**, 785 (2010); 10.1063/1.3499242

[On a variational principle for Beltrami flows](#)

*Phys. Fluids* **22**, 074102 (2010); 10.1063/1.3460297

[Two-wave structure of liquid film and wave interrelation in annular gas-liquid flow with and without entrainment](#)

*Phys. Fluids* **21**, 061701 (2009); 10.1063/1.3151999

[Solitary waves on inclined films: Flow structure and binary interactions](#)

*Phys. Fluids* **14**, 1082 (2002); 10.1063/1.1449465

---



## Kelvin waves with helical Beltrami flow structure

Rafael González,<sup>1,a)</sup> Gustavo Sarasua,<sup>2,b)</sup> and Andrea Costa<sup>3,c)</sup>

<sup>1</sup>*Departamento de Física FCEyN, Universidad de Buenos Aires, Buenos Aires, Argentina*  
and *Departamento de Desarrollo Humano, Universidad Nacional de General Sarmiento, Buenos Aires, Argentina*

<sup>2</sup>*Instituto de Física, Facultad de Ciencias, Universidad de la República, Montevideo, Uruguay*

<sup>3</sup>*Instituto de Astronomía Teórica y Experimental, Córdoba and Instituto de Astronomía y Física del Espacio, Buenos Aires, Argentina*

(Received 18 July 2007; accepted 18 December 2007; published online 27 February 2008)

In this work we show that when an inviscid axisymmetric Rankine flow experiences a soft expansion, rotating Kelvin waves can be excited. Downstream of the region where the expansion occurs (the transition region) the resulting flow can be expressed as the addition of a Rankine and a Beltrami flow. The Beltrami constant is determined from the Rankine upstream flow, and the helix pitch of the  $n=1$  mode results from the boundary conditions downstream. Finally, a discussion of the process leading to oscillatory flow and a conjecture about the topological background that sustains the Beltrami flow structure are offered. © 2008 American Institute of Physics.

[DOI: 10.1063/1.2840196]

### I. INTRODUCTION

The problem of the structural modification of a vortex in an axisymmetric swirling flow passing from an upstream cylindrical tube to a downstream one, through a transition expansion region, was historically related to two kinds of flows in the downstream region: The formation of a vortex breakdown or to an oscillatory flow.<sup>1,2</sup> The formation of helical structures<sup>3,4</sup> was of special practical and theoretical interest.

In previous works<sup>5,6</sup> we have studied some characteristics of this particular flow using the vortex filament solution. In this case, we focus on the study of the oscillatory flow and its connection with the features of the upstream flow. In doing so, our departure point is the well established Batchelor's analysis of the swirling flow.<sup>1</sup> This author took a Rankine flow upstream of an inviscid fluid and found the form of the steady Euler equations for the whole fluid field and the corresponding solutions for the downstream region. We show that the flow in transition and downstream regions is a Beltrami flow in a rotating and translating frame. As this resulted in a main characteristic of the overall flow, the consideration of this type of feature for the fluid is justified, more than assumed, as a simplification of the problem.<sup>4,7,8</sup> We also discuss deeper derivations of this result.

Dritschel<sup>7</sup> studied helical symmetric rotating waves in a cylindrical tube with the assumption of a Beltrami flow. He established that Lord Kelvin's mathematical expressions of 1880, obtained in terms of Bessel functions<sup>9</sup> for the linear stability of a rigidly rotating flow in a pipe, are exact solutions of the Euler equations. Other works assuming the Beltrami flow hypothesis are not conclusive concerning the physical background which it is supposed to be. Here, we show that the Rankine flow determines the formation of downstream Beltrami flows. Still, we discuss the role that the

topology plays in two important aspects, i.e., the frozen of the vorticity lines in an inviscid fluid, and the concept of helicity introduced in hydrodynamics by Moffatt.<sup>10,11</sup> At the same time, we argue about the possible origin of the structural change of the vortex, in the bifurcation of the basic flow.

We organize the sections as follows: In Sec. II we write the basic axisymmetric flow equations and show that in the transition and downstream regions they represent a Rankine plus a Beltrami flow field. In Sec. III, we introduce linear normal modes and show that helical rotating waves develop as a Beltrami flow, for a particular relationship between the frequency of the modes and the angular speed of the Rankine flow. In Sec. IV, we establish the boundary conditions downstream and we obtain the pitch of the helix for the  $n=1$  mode. In Sec. V a discussion in relation to the breaking of symmetry of the axisymmetric flow is presented and a conjecture regarding the relationship between the topology of the flow and the Beltrami condition is made.

### II. BASIC AXISYMMETRIC FLOW

We consider an inviscid fluid with a Rankine upstream flow scenario schematically shown in Fig. 1. In cylindrical coordinates the fluid is described as

$$v_{\theta} = \Omega r, \quad v_z = U_0, \quad v_r = 0 \quad \text{for } 0 \leq r \leq a_0, \quad (1)$$

$$v_{\theta} = \frac{\Omega a_0^2}{2\pi r}, \quad v_z = U_0, \quad v_r = 0 \quad \text{for } b_0 > r > a_0, \quad (2)$$

where  $\Omega$ ,  $U_0$ , and  $a_0$  are constants,  $a_0$  is the radius of the rotational core, and  $b_0$  is the radius of the inlet stream.

The upstream flow around the core is potential, and is  $\boldsymbol{\omega} = \nabla \times \mathbf{v} = 0$ . The Kelvin circulation theorem assures that the flow in the transition and downstream regions is also potential. Thus, for the whole structure we can separate the flow in a rotational zone (corresponding to the core), and an irrotational

<sup>a)</sup>Electronic mail: rgonzale@ungs.edu.ar; rgonzale@df.uba.ar.

<sup>b)</sup>Electronic mail: sarasua@fisica.edu.uy.

<sup>c)</sup>Electronic mail: acosta@mail.oac.uncor.edu; costa@iafe.uba.ar.

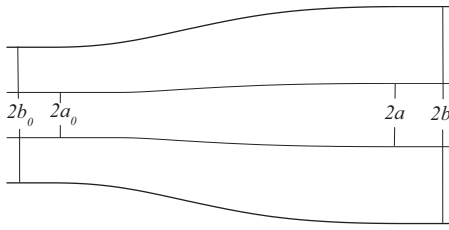


FIG. 1. Cylindrical tube with a perfect incompressible flow and a rotational core.  $b_0$  is the radius in the upstream region,  $b$  is the downstream radius. A soft transition region lays in between. The steady Rankine vortex in the upstream region has a core of radius  $a_0$ . Downstream the flow is either a steady axisymmetric flow with a rotational core radius  $a$  or a periodic flow with helical symmetry (not shown).

tional one corresponding to the potential flow.<sup>12</sup> On account of the mass conservation and the axisymmetry, we may introduce the stream function in the form

$$v_z = \frac{1}{r} \frac{\partial \psi}{\partial r}, \quad v_r = -\frac{\partial \psi}{\partial z}, \quad (3)$$

and the Euler equations are written as

$$\mathbf{v} \times \boldsymbol{\omega} - \frac{\partial \mathbf{v}}{\partial t} = \nabla H, \quad H = \frac{1}{2} \mathbf{v}^2 + \frac{p}{\rho}, \quad (4)$$

where  $H$  is the total head function. Thus, for the axisymmetric flow the constancy of the circulation  $C = r v_\theta$  is guaranteed. When the flow is steady, both the circulation and the total head are functions of the stream function, and the following relations are verified for the whole flow field:<sup>1</sup>

$$\omega_z = v_z \frac{dC}{d\psi}, \quad \omega_r = v_r \frac{dC}{d\psi}, \quad \frac{\omega_\theta}{r} = \frac{C}{r^2} \frac{dC}{d\psi} - \frac{dH}{d\psi}. \quad (5)$$

The upstream flow described by Eq. (1) determines linear relations of  $C(\psi)$  and  $H(\psi)$  for the whole rotational zone with  $\psi$ ,

$$C(\psi) = \frac{2\Omega}{U_0} \psi, \quad H(\psi) = \frac{1}{2} U_0^2 + \frac{2\Omega}{U_0} \psi. \quad (6)$$

Thus, from Eqs. (5) and (6), the following relations are obtained:

$$\omega_z = \gamma v_z, \quad \omega_r = \gamma v_r, \quad \omega_\theta = \gamma(v_\theta - \Omega r), \quad \text{with } \gamma = \frac{2\Omega}{U_0}. \quad (7)$$

As can be seen from Eq. (7), while the upstream rotational zone is described with a Rankine flow of vorticity  $\boldsymbol{\omega}_R = 2\Omega \mathbf{z}$ , the transition and downstream rotational zones can be described as the joint contribution of a Rankine flow  $\mathbf{v}_R$  plus a Beltrami one  $\mathbf{v}_B$ , and is

$$\mathbf{v} = \mathbf{v}_R + \mathbf{v}_B, \quad \boldsymbol{\omega} = \boldsymbol{\omega}_R + \boldsymbol{\omega}_B, \quad \boldsymbol{\omega}_B = \nabla \times \mathbf{v}_B = \gamma \mathbf{v}_B. \quad (8)$$

In fact, taking

$$v_z = U_0 + v_{Bz}, \quad v_r = v_{Br}, \quad v_\theta = \Omega r + v_{B\theta}, \quad (9)$$

from Eqs. (7) and (9), we derive Eq. (8).

Therefore, the main effect of the expansion is to produce a Beltrami flow superimposed to the Rankine one with the

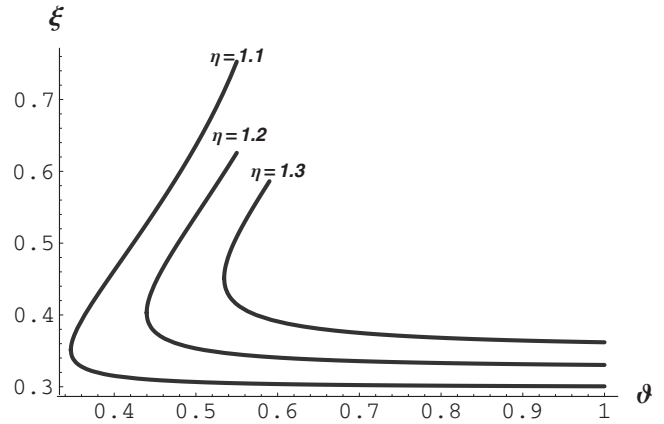


FIG. 2. Expansion radius of the core downstream  $\xi = a/a_0$  as a function of the Rossby number  $\vartheta$ .  $\eta = b/b_0$  is the expansion parameter (the values where taken from experimental research data, Ref. 3);  $\iota = a_0/b_0 = 0.272$ . The lower branch of each curve is stable and the upper one is unstable.  $\vartheta_c$ , the critical Rossby number value corresponds to the joint point.

Beltrami constant  $\gamma$  determined by the associated Rankine flow upstream. Moreover, the potential flow of the irrotational zone can be seen as a Beltrami flow with the eigenvalue  $\gamma_{\text{irrot}} = 0$ . In the downstream region the conservation laws for the axisymmetric solution give<sup>1,6</sup>

$$v_\theta = \Omega r + \gamma A J_1(\gamma r), \quad v_z = U_0 + \gamma A J_0(\gamma r), \quad (10)$$

$$v_r = 0 \quad \text{for } 0 \leq r \leq a,$$

$$v_\theta = \frac{\Gamma}{2\pi r}, \quad v_z = B U_0, \quad v_r = 0 \quad \text{for } b > r > a \quad (11)$$

as

$$A = \frac{U_0(a_0^2 - a^2)}{2a J_1(\gamma a)}, \quad B = \frac{(b_0^2 - a_0^2)}{(b^2 - a^2)}, \quad \gamma = \frac{2\Omega}{U_0}. \quad (12)$$

$a$  and  $b$  are the parameters of the downstream region (see Fig. 1).  $a$  is determined from the equation

$$\frac{(b_0^2 - a_0^2)}{(b^2 - a^2)} = 1 + \frac{\gamma(a_0^2 - a^2)}{2a J_1(\gamma a)} J_0(\gamma a), \quad (13)$$

which was obtained using the condition that the axial speeds are the same at  $r = a$ .

Equation (13) in a dimensionless form is written as

$$\frac{(1 - \iota^2)}{(\eta^2 - \xi^2)} = 1 + \frac{1}{\vartheta} \frac{(\iota^2 - \xi^2)}{\xi} \frac{J_0\left(\frac{2}{\vartheta} \xi\right)}{J_1\left(\frac{2}{\vartheta} \xi\right)}, \quad (14)$$

where  $\eta = b/b_0$  is the expansion parameter,  $\xi = a/a_0$  is the nondimensional expanded vortex radius,  $\iota = a_0/b_0$ , and  $\vartheta = U_0/\Omega b_0$  are the Rossby numbers, with  $U_0$  as the axial speed.

In Fig. 2 we plot the expanded vortex radius as a function of the Rossby number for different expansion parameters. As it was already pointed out in a previous work,<sup>6</sup> each line has two branches, an upper unstable one and a lower

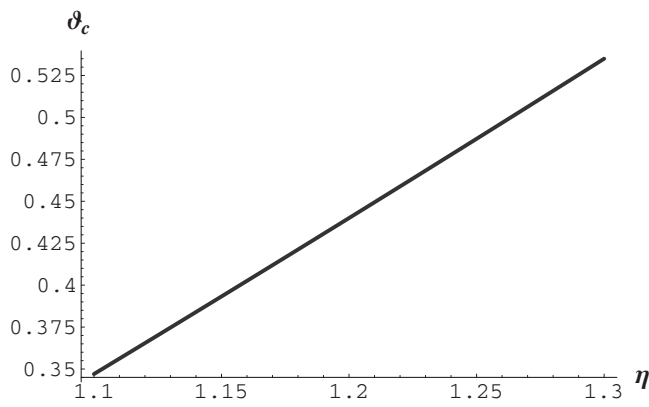


FIG. 3. Dependence of the critical Rossby number  $\vartheta_c$  on the expansion parameter  $\eta$ , for  $\iota=0.272$ .

stable branch. The point where the two branches—of different stability—join corresponds to the critical Rossby number  $\vartheta_c$ . Thus, a saddle-node bifurcation is obtained. When  $\vartheta < \vartheta_c$  the axisymmetric solutions Eqs. (10) and (11), are no longer possible and a breakdown can appear. Therefore, only when  $\vartheta > \vartheta_c$  the lower branch solution can support perturbed oscillations. The figure shows that the value of  $\vartheta_c$  grows with  $\eta$  which is also shown in Fig. 3. This means that when  $\eta$  is increased, the loss of the axisymmetric solution occurs at a lower angular speed  $\Omega$ . A necessary condition for these axisymmetric solutions to hold, which is satisfied by the flows considered here, is that reversal axial flows are not allowed all over the transition expansion region.<sup>1</sup>

Figure 4 shows the dependence of the expansion radius as a function of the Rossby number for different values of  $\iota$ , the upstream vortex radius. Note that the parameter  $\vartheta_c$  increases with  $\iota$ , and  $\iota=0.272$  corresponds to the observational value as stated in Ref. 3.

### III. HELICAL FLOW

We take infinitesimal perturbations of helical symmetry in the downstream flow, i.e., with velocities and pressure perturbations, as

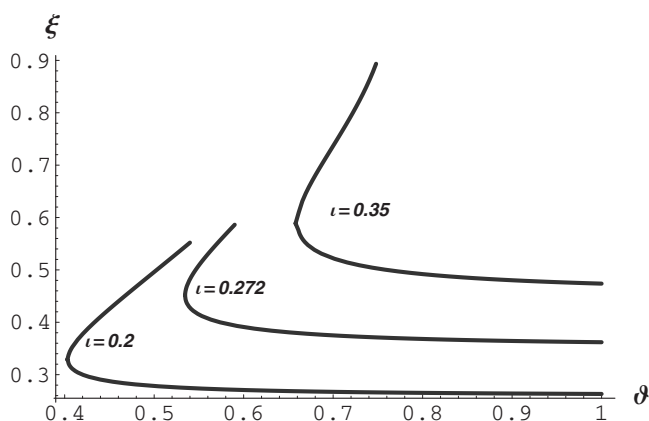


FIG. 4. Expansion radius of the core downstream  $\xi = a/a_0$  as a function of the Rossby number  $\vartheta$ , for the expansion parameter  $\eta=1.3$  and vortex radius  $\iota=0.2, 0.272$ , and  $0.35$ .

$$\{\delta v_r, \delta v_\theta, \delta v_z, \delta p\} = \{f(r), g(r), h(r), \pi(r)\} e^{in\phi - i\sigma t}, \quad (15)$$

where  $\phi = \theta - kz$  is the helical coordinate with the helix pitch  $k$ , and  $\sigma$  is the frequency of the perturbation. Imaginary positive values of  $\sigma$  indicate growing perturbations in time and the instability of the basic flow. Thus, the linearization around the axisymmetric solution of the Euler equations take a downstream form of the type

$$ikn\pi = ih \left( \frac{nv_\theta}{r} - knv_z - \sigma \right) + f \frac{dv_z}{dr}, \quad (16)$$

$$-\frac{d\pi}{dr} = if \left( \frac{nv_\theta}{r} - knv_z - \sigma \right) - 2g \frac{v_\theta}{r}, \quad (17)$$

$$-\frac{in\pi}{r} = ig \left( \frac{nv_\theta}{r} - knv_z - \sigma \right) + f \left( \frac{dv_\theta}{dr} + \frac{v_\theta}{r} \right), \quad (18)$$

$$iknh = \frac{1}{r} \left( \frac{d(rf)}{dr} + ing \right), \quad (19)$$

where  $(v_\theta, v_r, v_z)$  are the velocity components of the basic flow. The linear stability of the basic flow is determined (taking into account boundary conditions) by the solutions of Eqs. (16)–(19) in the rotational and irrotational zones, i.e., solving the corresponding eigenvalue equation that relates  $\sigma$  to  $n$ .

Our aim is to show that there are some real values of  $\sigma$  for which the solutions of Eqs. (16)–(19) represent a helical Beltrami flow with perturbations of the form Eq. (15) corresponding to Kelvin waves that propagate in the axisymmetric core surrounded by an irrotational flow. We are also interested in the driving mechanism of these waves.

In order to solve Eqs. (16)–(19) in the rotational zone we choose

$$\sigma = n\Omega. \quad (20)$$

Note that if this condition is satisfied it can be easily verified that in the rotational downstream zone the solutions of Eqs. (16)–(19) associated with perturbations of the basic flow given by Eq. (10) match the Beltrami condition Eq. (7) and can be written as

$$f_{\text{rot}_n} = -iC_{\text{rot}_n} \left[ \frac{\mu_n J'_n(\mu_n r)}{k} - \frac{\gamma}{k^2 r} J_n(\mu_n r) \right], \quad (21)$$

$$g_{\text{rot}_n} = C_{\text{rot}_n} \left[ \frac{n}{kr} J_n(\mu_n r) - \frac{\mu_n \gamma}{k^2 n} J'_n(\mu_n r) \right], \quad (22)$$

$$h_{\text{rot}_n} = C_{\text{rot}_n} \frac{\mu_n^2}{k^2 n} J_n(\mu_n r), \quad (23)$$

where

$$\mu^2 = \gamma^2 - n^2 k^2. \quad (24)$$

On the other hand, and for the frequency of Eq. (20), the solutions of Eqs. (16)–(19), associated with basic flow perturbations in the irrotational downstream zone [see Eq. (11)], which satisfy the boundary condition  $\delta \mathbf{v}_{\text{irrot}}(r=b)=0$  can be written as

$$f_{\text{irrot}_n} = \left( \frac{i}{kn} \right) \frac{dh_{\text{irrot}_n}}{dr}, \quad (25)$$

$$g_{\text{irrot}_n} = - \frac{h_{\text{irrot}_n}}{kr}, \quad (26)$$

$$h_{\text{irrot}_n} = C_{\text{irrot}_n} \left[ I_n(nkr) - \frac{I'_n(nkb)}{K'_n(nkb)} K_n(nkr) \right]. \quad (27)$$

In the next section we will come back to the necessary matching conditions (for the  $n=1$  case) at the frontier of the rotational and the irrotational zones. Defining the angular coordinate  $\varphi = \phi - \Omega t$ , Eq. (15) represents a helical rotating wave. In the rotating frame with angular speed  $\Omega$ , the flow is steady. Therefore, the downstream flow for the rotational zone is

$$\mathbf{v}_{\text{rot}} = (0, \Omega r, U_0) + \left\{ \left[ 0, \gamma A J_1(\gamma r), \gamma A J_0(\gamma r) \right] + \sum_{n \geq 1} [f_{\text{rot}_n}(r), g_{\text{rot}_n}(r), h_{\text{rot}_n}(r)] e^{in\varphi} + \text{c. c.} \right\}, \quad (28)$$

while for the irrotational zone we have

$$\mathbf{v}_{\text{irrot}} = \left( 0, \frac{\Gamma}{2\pi r}, B U_0 \right) + \sum_{n \geq 1} [f_{\text{irrot}_n}(r), g_{\text{irrot}_n}(r), h_{\text{irrot}_n}(r)] e^{in\varphi} + \text{c. c.} \quad (29)$$

The first term of Eqs. (28) and (29) represents a Rankine flow. The second one represents a steady Beltrami flow in a frame turning with angular speed  $\Omega$ , with constants  $\gamma$  and  $\gamma_{\text{irrot}}=0$ , respectively. In fact, as it was shown by Chandrasekhar and Kendall<sup>13</sup> or by Barberio-Corsetti,<sup>14</sup> it is the solution of the equation  $\nabla \times \mathbf{v}_B = \gamma \mathbf{v}_B$  in cylindrical coordinates (or a force-free equation in the magnetic example). The coefficients of the expansion give the linear solution and are arbitrary, i.e., they satisfy Euler's equation around the equilibrium state.

Still, as was shown in Sec. II, for the transition and downstream regions in the axisymmetric case, the description of the flow requires the sum of a Rankine plus a Beltrami flow. This allows us to consider the driven helical Beltrami downstream flow in two steps: First, an axisymmetric Beltrami flow arises caused by the expansion, with the eigenvalue  $\gamma$  determined by the Rankine flow upstream, Eq. (7). Second, the perturbation of this axisymmetric Beltrami flow results in a helical Beltrami flow. The helical flow can be represented as the bifurcation via the diminishing of the Rossby number to a critical value from the axisymmetric base flow. Due to the fact that the principal features of the bifurcation arise from the disturbances starting at the critical point, we can obtain the helix pitch value at the downstream region from the linear boundary conditions. In order to give an account of the reasons why the Beltrami character of the flow remains downstream of the expansion region, we study the special case of the  $n=1$  mode. This mode is the principal mode resulting from the experimental research of Ref. 3.

#### IV. BOUNDARY CONDITIONS AND HELIX PITCH FOR THE $n=1$ MODE

To find the helix pitch  $k$  as a function of the Rossby number for the basic flow cases of Sec. II we apply the boundary conditions at the frontier between the rotational and the irrotational zones to the  $n=1$  mode of the flows given by Eqs. (28) and (29). To this aim we follow the procedure performed in a previous work.<sup>6</sup> Writing the perturbed core radius as  $r = a + \Delta e^{in\phi - i\sigma t}$ , after linearizing, the continuity of the pressure across this boundary implies

$$\left. \frac{dP_{0,\text{irr}}}{dr} \right|_{r=a} \Delta + \pi_{\text{irr}}(a) = \left. \frac{dP_{0,\text{rot}}}{dr} \right|_{r=a} \Delta + \pi_{\text{rot}}(a). \quad (30)$$

On the other hand, the fact that the surface  $r=a + \Delta e^{in\phi - i\sigma t}$  moves with the fluid gives the kinematics condition

$$\frac{D\Delta}{Dt} = \frac{\partial \Delta}{\partial t} + (\mathbf{V}_0 \cdot \nabla) \Delta = \delta v_r, \quad (31)$$

which must be satisfied on both sides of the surface, with  $\mathbf{V}_0$  as the basic flow. Then, taking into account Eqs. (10), (11), (21)–(23), and (25)–(27) and the resonant condition Eq. (20) replaced in Eqs. (30) and (31) we obtain the equation for  $k$  as an implicit function of the Rossby number  $\vartheta$ , which in terms of the dimensionless variables defined in Eq. (14) results in

$$\begin{aligned} & \frac{n}{k} \left( -\frac{1}{\vartheta} + \frac{1}{\vartheta} \frac{\iota^2}{\xi^2} - k \frac{1-\iota^2}{\eta^2 - \xi^2} \right)^2 \tilde{f}_{\text{rot}_n}(\xi) \tilde{h}_{\text{irrot}_n}(\xi) + \tilde{f}_{\text{irrot}_n}(\xi) \\ & \times \left\{ \frac{\iota^2(\iota^2 - 1)}{\vartheta^2 \xi^3} \tilde{f}_{\text{rot}_n}(\xi) + n \left( \frac{1}{\vartheta} \frac{\iota^2 - \xi^2}{\xi^2} - k \frac{1-\iota^2}{\eta^2 - \xi^2} \right) \right. \\ & \times \left[ \left( \frac{1}{\vartheta} \frac{\iota^2 - \xi^2}{\xi^2} - k \frac{1-\iota^2}{\eta^2 - \xi^2} \right) \frac{\tilde{h}_{\text{rot}_n}(\xi)}{k} \right. \\ & \left. \left. + \frac{2}{\vartheta^2} \frac{\iota^2 - \xi^2}{\xi^2} \frac{\tilde{f}_{\text{rot}_n}(\xi)}{kn} \right] \right\} = 0, \quad (32) \end{aligned}$$

where  $\tilde{f}, \tilde{g}, \tilde{h}$  are the nondimensional velocity components  $f, g, h$  given by Eqs. (21)–(23) and (25)–(27) in the rotational and the irrotational zones.

The helix pass is defined as the  $z$  length variation (for a given value of coordinate  $\phi$ ) when  $\theta$  changes an amount  $2\pi$ . In fact,  $\Delta\phi = \Delta\theta - k\Delta z$  if  $\Delta\phi=0$  and  $\Delta\theta=2\pi$  it results in the  $H_p = \Delta z = 2\pi/k$  helix pass. Thus, numerically solving Eq. (32), we obtain Figs. 5 and 6 for the pitch  $k$  and the helix pass  $H_p$ , respectively, as a function of the Rossby number for the mode  $n=1$ . From the figures we see that the helix pitch increases and the helix pass decreases with increasing expansion  $\eta$  and decreasing Rossby number  $\vartheta$ , respectively. For a definite Rossby number we obtain, in accordance with Eq. (24), an upper limit of the pitch due to the relation  $k \leq 2/\vartheta$ .

As seen, a saddle-node bifurcation of an axisymmetric flow occurs when  $\vartheta = \vartheta_c$ , and the basic flow disappears when  $\vartheta < \vartheta_c$ . Thus, when subject to infinitesimal helical perturbations of the form Eq. (15), helical rotating flows can arise if  $\vartheta > \vartheta_c$  together with the marginal stability of the lower

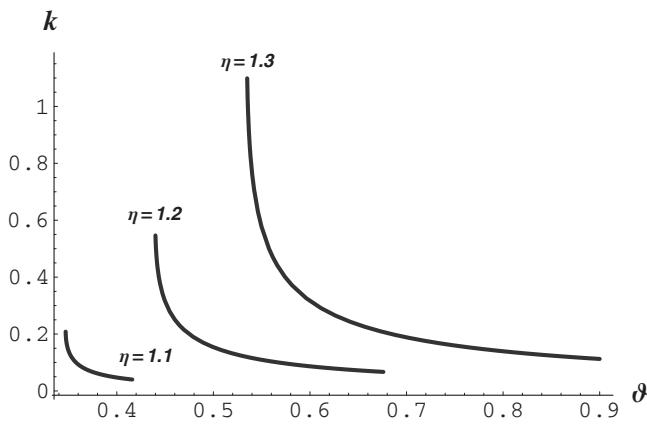


FIG. 5. Helix pitch  $k$  as a function of the Rossby number  $\vartheta$  for  $\eta$  values: 1.1, 1.2, and 1.3;  $\iota=0.272$  and the helical mode  $n=1$ .

branch of the basic axisymmetric flow. On the other hand, and for finite amplitude perturbations, the passage from axisymmetric flow to helical flow is also a bifurcation. Due to the rotating character this is a Hopf bifurcation whose Rossby critical value  $\vartheta_{cc}$  is  $\vartheta_{cc} > \vartheta_c$ .

As an example, to give account of this critical parameter, we can first consider the mode  $n=1$ . We see that most of the helix pass values result in one or two orders of magnitude greater than the unit length value. Also, our results correspond (the same order of magnitude) to the observed experimental values.<sup>3</sup> So, taking these results into account, we chose the value  $H_p=10$  as a limit parameter of the calculus. Secondly, in Eq. (15) we took the frequency  $\sigma=n\Omega+is$  with  $s \rightarrow 0$ . Figure 7 shows the dependence of  $s$  with the parameter  $\vartheta$ , note that  $\vartheta_{cc} \approx 0.565$  due to the fact that if  $\vartheta < 0.565$ , then  $s > 0$  (unstable case), and that  $s < 0$  when  $\vartheta > 0.565$  (stable). Thus,  $s \propto \text{cte}(\vartheta - \vartheta_{cc})$  near  $\vartheta_{cc}$ .

## V. SUMMARY AND DISCUSSION

In what follows, we summarize the main results of our work and we present a discussion in relation to the formation of RKW and the Beltrami flow structure.

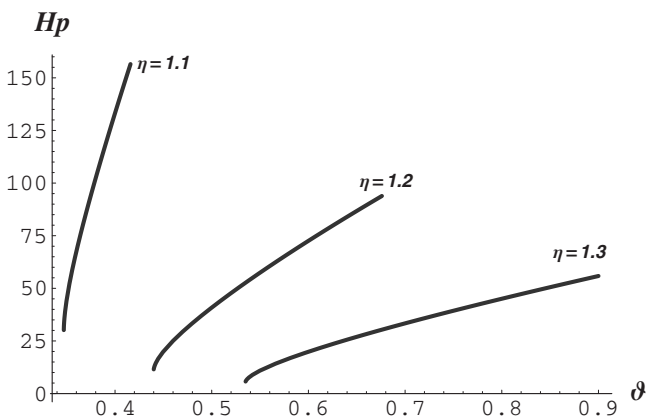


FIG. 6. Helix pass as a function of the Rossby number  $\vartheta$  for  $\eta$  values: 1.1, 1.2, and 1.3;  $\iota=0.272$  and the helical mode  $n=1$ .

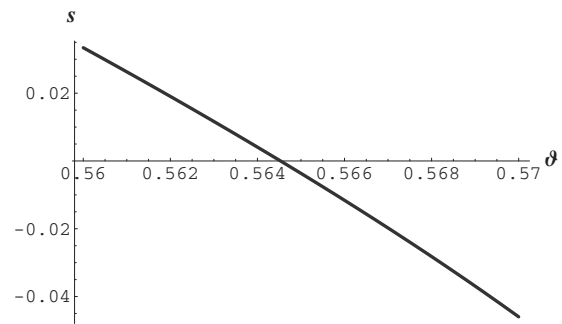


FIG. 7. Imaginary part of the frequency  $\sigma=n\Omega+is$  as a function of the Rossby number  $\vartheta$  for  $\eta=1.3$ ,  $\xi=0.4$ ,  $H_p=10$ ,  $\iota=0.272$  and the helical mode  $n=1$ . From this figure we see that  $\vartheta_{cc} \approx 0.565$ .

(i) A Rankine upstream flow subject to a smooth expansion (see Fig. 1) turns to an axisymmetric flow that can be expressed as the addition of a Rankine and a Beltrami flow in the rotational zone at the transition and downstream regions. The value of the Beltrami eigenvalue  $\gamma=2\Omega/U_0$  is determined by the Rankine parameters  $\Omega$  and  $U_0$ ; in nondimensional variables the eigenvalue is  $2/\vartheta$ , with  $\vartheta$  the Rossby number.

(ii) As shown in Fig. 2, we obtain a representation of the expanded vortex radius downstream in terms of a two branched function of the Rossby number: An upper unstable branch and a lower stable one joining at the critical Rossby number  $\vartheta_c$ , where a saddle-node bifurcation takes place. When  $\vartheta < \vartheta_c$  the axisymmetric solutions are lost and a breakdown can appear. Therefore, to support perturbations of the lower branch solution the flow has to fulfill the relation  $\vartheta > \vartheta_c$ . The value of  $\vartheta_c$  grows with the expansion parameter  $\eta$ .

(iii) The perturbations become Kelvin waves with a helical Beltrami flow structure if the resonant condition  $\sigma=n\Omega$  is satisfied by the frequency  $\sigma$ . The basic axisymmetric flow is marginally stable for infinitesimal helical perturbations.

(iv) A main result obtained is that, as in the case of the axisymmetric flow, the eigenvalue  $\gamma=2\Omega/U_0$  is determined by the Rankine parameters  $\Omega$  and  $U_0$ .

(v) We determined the helix pitch  $k$  and the helix pass  $H_p$  as a function of the Rossby number represented in Figs. 5 and 6, respectively, for the mode  $n=1$  via the application of matching conditions between downstream rotational and irrotational zones and infinitesimal helical perturbations with the resonant condition Eq. (20). We defined the parameter  $\vartheta_{cc}$  as the critical Rossby number; as can be seen from Fig. 7, if  $\vartheta=\vartheta_{cc}$  a Hopf bifurcation takes place. For this value, the flow is marginally stable; it becomes unstable if  $\vartheta < \vartheta_{cc}$  and stable if  $\vartheta > \vartheta_{cc}$ .

(vi) From Fig. 5 we also note that the helix pitch grows with the expansion parameter  $\eta$  and decays with the Rossby number  $\vartheta$ .

(vii) Helical rotating waves take place in the range  $(\vartheta_c, \vartheta_{cc})$ . In the example of Sec. IV the interval is  $(0.535, 0.565)$ .

We now have elements to discuss about the structural

features that led to (a) the formation of helical Kelvin waves and (b) the fact that these waves are of a Beltrami flow type.

(a) The scenario: When  $\vartheta > \vartheta_{cc}$ , the Rankine flow passing through the expansion region preserves its axisymmetric character. The expansion produces a Beltrami axisymmetric flow of eigenvalue  $\gamma = 2\Omega/U_0$  determined by the upstream Rankine flow. If  $\vartheta$  is decreased the same configuration is maintained until the critical value  $\vartheta_{cc}$  is reached. From a frame system turning with  $\Omega$  and translating with  $U_0$ , this value corresponds to the occurrence of a bifurcation—from a Beltrami axisymmetric flow to a Beltrami helical flow—produced by helical perturbations. The occurrence of a Hopf bifurcation for a marginally stable axisymmetric solution implies that, on the one hand, infinitesimal helical perturbations are sustained by the axisymmetric solutions when  $\vartheta = \vartheta_{cc}$ , i.e., the saddle-node bifurcation controls the dynamic in the subspace of axisymmetric solutions. For finite amplitudes on the other hand the Hopf bifurcation controls the angular stability in the orthogonal subspace. A main feature of this flow is that the corresponding eigenvalue is always the same,  $\gamma$ . Thus the whole new flow can be represented again by the addition of a Rankine and a Beltrami flow. As was seen from the linear approximation the superposition of modes is possible because modes of higher wave-number order have the same eigenvalue,  $\gamma$ . Therefore, bifurcations other than the one associated with mode  $n=1$  could have a different critical parameter  $\vartheta_{cc}$ , but they will require an identical scenario. Kelvin waves with helical Beltrami flow structure are obtained while  $\vartheta$  decreases until a critical value  $\vartheta_c$  is reached, giving rise to the possibility of a vortex breakdown.<sup>1</sup>

(b) About the reasons why a Beltrami flow is a final state of the axisymmetric and helical symmetry cases.

The Woljter Theorem.<sup>15</sup> Woljter has introduced the concept of helicity in the context of the ideal magnetohydrodynamics, and proved that a force-free equilibrium (the analogous of the Beltrami one) can be obtained from a variational principle. In fact, he showed that this equilibrium configuration results from minimizing the magnetic energy restricted to the helicity conservation. The force-free magnetic equilibrium is expressed as  $\nabla \times \mathbf{B} = \alpha \mathbf{B}$ , with  $\mathbf{B}$  the magnetic field,  $\alpha$  constant and the helicity defined as the integral  $\int \mathbf{A} \cdot \mathbf{B} dV$  over the plasma volume, where  $\mathbf{A}$  is the potential vector  $\nabla \times \mathbf{A} = \mathbf{B}$ .

Moffatt<sup>10</sup> was the first to introduce the concept of helicity in hydrodynamics, defined as  $\int \mathbf{v} \cdot \boldsymbol{\omega} dV$ . Moreover, it was proved<sup>11</sup> that for the ideal hydrodynamics, the helicity that expresses topological properties of the flow, is conserved.

We present here a conjecture that will be the subject of a future research. Focusing on the topological analogy between the behavior of the magnetic field, in ideal magnetohydrodynamics, and the vortex field, in ideal hydrodynamics, we note that: a direct consequence of the Kelvin circulation theorem is that as the magnetic lines, the vortex lines are frozen to the fluid. First, in analogy to the magnetic energy  $M = \int B^2 dV$  of Woljter's theorem we can define the enstrophy as the integral over a fluid volume of the square of the vorticity  $\Phi = \int \omega^2 dV$ . We assume a null surface integral at the boundary. The Appendix shows that the Beltrami flow is an extreme of the enstrophy subject to the helicity conservation.

The enstrophy variation is not affected if a frame with a uniform rotation and a uniform translation is adopted. In the magnetic case the physical conditions that lead to the force-free equilibrium are the frozen of the magnetic field lines to the fluid and the helicity conservation. Then the variational principle leads to the equilibrium via the minimization of the magnetic energy. Both physical conditions are present in our case. So, this *topological analogy* suggests the conjecture that in a frame with uniform rotation and translation where this flow is steady, both conditions lead to the Beltrami equilibrium. The extreme of the enstrophy is the topological analog of the magnetic energy. The conjecture resembles the Kelvin's variational principle<sup>16</sup> for a two-dimensional fluid in the sense that considers the steady states in the same type of frame too.

Although the condition  $\boldsymbol{\omega}_B = \nabla \times \mathbf{v}_B = \gamma \mathbf{v}_B$  is determined by making zero this first variation of the enstrophy, the stability of the equilibrium is not guaranteed. It requires  $\delta^2 \Phi \geq 0$  to assure a minimum value of  $\Phi$ . Nevertheless, we anticipate arguments in favor of stability. The variational principle gives all possible solutions of the Euler equations. When the helicity is conserved, the solution is the Beltrami flow for a given eigenvalue. In our case, the eigenvalue  $\gamma$  is determined previously by the Rankine flow. Then both, the *helicity conservation*, and the *given  $\gamma$  eigenvalue* determine the Beltrami flow downstream. However, some final features are determined (e.g., the helix pitch) by equilibrium parameters and boundary conditions. While  $\vartheta > \vartheta_{cc}$  the final equilibrium is the Beltrami axisymmetric flow. Yet, when  $\vartheta$  is in the range  $(\vartheta_c, \vartheta_{cc})$  the final state is the rotating helical Beltrami flow.

On the other hand, the axisymmetric Beltrami flow corresponds to the stable axisymmetric steady solution. So, as Batchelor pointed out, axisymmetric waves of finite amplitude can arise. Nevertheless, the helical Beltrami perturbations lead to marginal stability, whenever the eigenvalue of the perturbations is *the same  $\gamma$  eigenvalue* as the basic Beltrami one. This marginal stability holds for infinitesimal amplitude perturbations but when  $\vartheta$  reaches the critical value  $\vartheta_{cc}$  the finite amplitudes produce a Hopf bifurcation. The final state is a rotating wave with *Beltrami flow structure of eigenvalue  $\gamma$* . We conjecture that when a transition between steady states of different symmetries occur, stability against infinitesimal perturbations is guaranteed if the transition relates a Beltrami state to another of the same eigenvalue. In our case, for finite amplitude the dynamic is dominated by the equilibrium characteristics: the saddle-node bifurcation by  $\vartheta > \vartheta_{cc}$  and the Hopf bifurcation by  $\vartheta < \vartheta_{cc}$ . However, for both, the axisymmetric and the helical symmetric cases, when  $\vartheta > \vartheta_c$  the final state is a flow with Beltrami field structure. Some authors<sup>4</sup> have discussed the reasons to assume a Beltrami flow. Our conjecture proposes that when a Rankine flow is assumed as the ideal flow in a tube, the most natural final state that follows the perturbations is a Beltrami flow.

## ACKNOWLEDGMENTS

We are very grateful to Professor Fernando Minotti for his valuable comments. This paper is dedicated to the memory of our professor and guide Constantino Ferro Fontán, and also to the memory of our colleague and friend Aníbal Sicardi Schifino.

## APPENDIX: VARIATIONAL DERIVATION OF THE EQUILIBRIUM BELTRAMI FLOW

Let  $\Phi$  be the enstrophy defined as

$$\Phi = \int \omega^2 dV \quad (\text{A1})$$

in the domain  $D$  with the conditions that  $\hat{n} \cdot \boldsymbol{\omega} = 0$  and  $\hat{n} \cdot \mathbf{v} = 0$  on  $\partial D$ . And let  $\int \mathbf{v} \cdot \boldsymbol{\omega} dV$  be the helicity with the condition

$$\int \mathbf{v} \cdot \boldsymbol{\omega} dV = \text{constant}. \quad (\text{A2})$$

Taking the first variation of  $\Phi$  subject to Eq. (A2) and introducing the constant Lagrangian multiplier  $\gamma$ , we obtain

$$\begin{aligned} \delta\Phi = \int & 2\{(\nabla \times \mathbf{v}) \cdot (\nabla \times \delta\mathbf{v}) - \gamma[\delta\mathbf{v} \cdot (\nabla \times \mathbf{v}) \\ & + \mathbf{v} \cdot (\nabla \times \delta\mathbf{v})]\} dV \\ = 0. \end{aligned} \quad (\text{A3})$$

Integrating by parts and discarding the surface integrals we obtain

$$\nabla \times \boldsymbol{\omega} = \gamma \boldsymbol{\omega}. \quad (\text{A4})$$

Equation (A4) corresponds to the vorticity field,

$$\boldsymbol{\omega} = \gamma \mathbf{v} + \nabla \psi, \quad \nabla^2 \psi = 0 \text{ in } D, \quad \hat{n} \cdot \nabla \psi = 0 \text{ on } \partial D. \quad (\text{A5})$$

The condition Eq. (A5) for  $\psi$  gives

$$\psi = 0, \quad \boldsymbol{\omega} = \gamma \mathbf{v}, \quad (\text{A6})$$

completing the demonstration.

<sup>1</sup>G. K. Batchelor, *An Introduction to Fluids Dynamics* (Cambridge University Press, Cambridge, 1967).

<sup>2</sup>B. Benjamin, "Theory of the vortex breakdown phenomenon," *J. Fluid Mech.* **14**, 593 (1962).

<sup>3</sup>R. Guarga and J. Cataldo, "A theoretical analysis of symmetry loss in high Reynolds swirling flows," *J. Hydraul. Res.* **31**, 35 (1993).

<sup>4</sup>S. V. Alekseenko, P. A. Kuibin, L. Okulov, and S. I. Shtork, "Helical vortices in swirl flow," *J. Fluid Mech.* **382**, 195 (1999).

<sup>5</sup>L. G. Sarasua, A. C. Sicardi-Schifino, and R. Gonzalez, "The stability of steady, helical vortex filaments in a tube," *Phys. Fluids* **11**, 1096 (1999).

<sup>6</sup>L. G. Sarasua, A. C. Sicardi-Schifino, and R. Gonzalez, "The development of helical vortex filaments in a tube," *Phys. Fluids* **17**, 044104 (2005).

<sup>7</sup>D. G. Dritschel, "Generalized helical Beltrami flows in hydrodynamics and magnetohydrodynamics," *J. Fluid Mech.* **222**, 525 (1991).

<sup>8</sup>M. J. Landman, "On the generation of helical waves in circular pipe flow," *Phys. Fluids A* **2**, 738 (1990).

<sup>9</sup>Lord Kelvin, "Vibrations of a columnar vortex," *Philos. Mag.* **10**, 155 (1880).

<sup>10</sup>H. K. Moffatt, "The degree of knottedness of tangled vortex lines," *J. Fluid Mech.* **36**, 17 (1969).

<sup>11</sup>H. K. Moffatt and A. Tsinober, "Helicity in laminar and turbulent flow," *Annu. Rev. Fluid Mech.* **24**, 281 (1992).

<sup>12</sup>From now onwards we use the word "zone" for the potential and nonpotential parts of the fluid and the word "region" to distinguish the upstream, transition, and downstream parts of the fluid.

<sup>13</sup>S. Chandrasekhar and P. C. Kendall, "On force-free magnetic field," *Astrophys. J.* **126**, 457 (1957).

<sup>14</sup>P. Barberio-Corsetti, "Force-free helical equilibria," *Plasma Phys.* **15**, 1131 (1973).

<sup>15</sup>L. Woljter, "A theorem on force-free magnetic fields," *Proc. Natl. Acad. Sci. U.S.A.* **44**, 489 (1958).

<sup>16</sup>P. G. Saffman, *Vortex Dynamics* (Cambridge University Press, Cambridge, 1992).